# Investigation of coupled control of gas accumulation and spontaneous combustion in the goaf of coal mine

Ke Gao, Zhipeng Qi, Jinzhang Jia, Shengnan Li, Zeyi Liu, and Zimeng Liu

## COLLECTIONS

View Online          Export Citation          CrossMark

## ARTICLES YOU MAY BE INTERESTED IN

**AIP Advances**
Mathematical Physics Collection          READ NOW

# Investigation of coupled control of gas accumulation and spontaneous combustion in the goaf of coal mine

View Online    Export Citation    CrossMark

Ke Gao,[1,2,a] Zhipeng Qi,[1] Jinzhang Jia,[1,2] Shengnan Li,[1] Zeyi Liu,[1] and Zimeng Liu[1]

AFFILIATIONS

[1] College of Safety Science and Engineering, Liaoning Technical University, Huludao, Liaoning 125105, China
[2] Key Laboratory of Mine Thermo-motive Disaster and Prevention, Ministry of Education, Huludao, Liaoning 125105, China

[a] Author to whom correspondence should be addressed: gaoke@lntu.edu.cn

ABSTRACT

To control the gas accumulation and spontaneous combustion in goafs of coal mines, many measures such as airflow volume at the working face, gas extraction, and nitrogen injection in goafs have been taken. However, the principles of these measures contradict when controlling two hazards simultaneously. It is necessary to understand how the flow field in goafs is influenced by these measures. In this study, a mathematical model of the flow field in a goaf behind a u-type mechanized working face is established using the theory of porous media. The flow field in a goaf with the risk of gas accidents and spontaneous combustion was analyzed for different controlling measures. Taking the Daxing coal mine in Liaoning Province as an example, the main parameters, such as airflow volume, gas extraction, and nitrogen injection, were optimized based on the simulation results. These results are of great significance for the coupled control of gas accumulation and spontaneous combustion in goafs of coal mines.

## I. INTRODUCTION

Disasters with gas accumulation and fire coupled together in goafs can easily occur[1–3] because of poor handling of the relationship between fire prevention and gas disasters, which is a prerequisite for preventing goaf disasters. A high caving space in thick coal seams is created by fully mechanized caving mining, resulting in more coal left in the goaf. High-intensity mining increases the intensity of gas desorption and emission, which requires a relatively large airflow at the working face, thus increasing the air leakage from the working face to the goaf, which increases the risk of spontaneous combustion in the goaf. Hence, the goaf is subject to the dual pressure of spontaneous combustion and gas accidents. This phenomenon is widespread in China, namely, the gas explosion in the goaf of the Babao coal mine in 2013, gas explosion in the goaf of the Tangyang coal mine in 2018, and fire in the goaf of the Qilianta coal mine in 2011. Therefore, the coupling mechanism and prevention of the spontaneous combustion and gas disasters in a goaf are still some of the major issues.

Correctly handling the relationship between fire prevention and gas disasters is a prerequisite for preventing goaf disasters.[4]

For controlling gas accumulation and spontaneous combustion simultaneously in a goaf, multiple measures, such as gas extraction, grouting, nitrogen injection, and air adjustment, have to be adopted together. However, the principles and methods of gas accumulation and spontaneous combustion prevention are inconsistent for two reasons: (1) gas extraction increases the air leakage in a goaf[5,6] and (2) although the width of the oxidation zone in a goaf is decreased by reducing the airflow volume at the working face, the possibility of gas accumulation is increased, which could result in excessive gas concentrations at the working face or the upper corner.[7,8] To avoid these problems in a goaf, a series of studies have been carried out. A number of influencing factors, including airflow,[9–11] the advancement of the working face,[12–14] gas extraction,[15–17] and nitrogen injection,[18,19] have been studied for controlling gas distribution and spontaneous combustion. As a result, a series of comprehensive measures for coal fire and gas accumulation prevention in a

goaf have been proposed.[20–22] However, these scientific and effective methods for controlling spontaneous combustion and gas disasters in a goaf still lack theoretical guidance.[23–25] An investigation of the coupled control of gas accumulation and spontaneous combustion in goafs of coal mines is of great importance and could provide a theoretical basis and technical support for controlling gas disasters and spontaneous combustion in coal mines.

## II. PERMEABILITY ANALYSIS AND EQUATION FOR THE FLOW OF A GOAF

### A. Governing equations for the goaf flow field

A goaf is a porous medium, and gas flows in the pores of the goaf. It is assumed that seepage, diffusion, and chemical reactions in a goaf are in steady-state, and the Soret and Dufour effects are ignored. The governing equations that describe the motion of the fluid flow in a goaf include a set of the Navier–Stokes equations, continuity equations, and any additional conservation equations, such as those for energy or species concentrations,[26–28]

$$\begin{cases} \dfrac{\delta \rho}{\delta t} + \dfrac{\delta}{\delta x_i}(\rho u_i) = S_m, \\[2mm] \dfrac{\delta}{\delta t}(\rho u_i) + \dfrac{\delta}{\delta x_j}(\rho u_i u_j) = -\dfrac{\delta P}{\delta x_i}, \\[2mm] C_e \dfrac{\delta T}{\delta t} + n\sigma_g V_i \dfrac{\delta T}{\delta x_i} = Q_s + \lambda_e \dfrac{\partial^2 T}{\partial x_i^2} + \dfrac{\delta \tau_{ij}}{\delta x_j} + \rho g_j + F_i, \\[2mm] \dfrac{\delta C}{\delta t} = D_d\, div(grad C) - V_i grad C + V(t), \end{cases} \quad (1)$$

where $\rho$ is the density (kg/m$^3$), $t$ is the time (s), $u$ is the velocity (m/s), $S_m$ is the gas source, including nitrogen and oxygen (kg/m$^3$ s), $P$ is the static pressure (Pa), $\tau$ is the stress tensor (N/m$^2$), $\rho g\, F$ is the gravity and external body force (N), $F$ includes the source attached to the model, such as porous media settings, $V_i$ is the velocity components in the $x$, $y$, and $z$ directions (m/s), $C_e$ is the effective heat capacity for the porous media (J/m$^3$ °C), $\lambda_e$ is the equivalent thermal conductivity for the porous media (W/m °C), $\sigma_s$ and $\lambda_s$ are the total equivalent heat capacity and thermal conductivity of the solid in the porous media, respectively, $\sigma_g$ and $\lambda_g$ are the total equivalent heat capacity and thermal conductivity of the gas in the porous media, respectively, $n$ is the porosity, $Q_s$ is the heat release from the oxidation of lost coal in the goaf (J/m$^3$ s), $C$ is the component concentration, $D_d$ is the diffusion coefficient of oxygen in the medium, (m$^2$/s), and $V(t)$ is the gas consumption or production volume for a gas concentration $C$.

### B. Physical model

This paper takes 702 working faces of the Daxing Coal Mine in Liaoning TieFa Co. Ltd. as the research object. In the working face, the fully mechanized caving mining technology and a U type ventilation system are adopted. The relative gas emission volume is 24.46 m$^3$/t. Spontaneous combustion easily takes place in the goaf where the shortest period is about 20 days. $C_2H_4$ and $C_2H_2$ were often detected in the goaf even if many measures were used. To control the gas and spontaneous combustion in the goaf simultaneously, these measuring parameters should be

optimized. The computational domain of the goaf is $300 \times 150 \times 100$ m$^3$, and the inclination angle of the working face is 15° (Fig. 1).

### C. Permeability coefficient

Permeability is defined as follows:[29–31]

$$K_p(x,y) = K_{p,min} + (K_{p,max} - K_{p,min})$$
$$\times \exp\left(-a_1 d_1\left(1 - \ell^{-\xi_1 a_0 b_0}\right)\right)(\xi_1 < 1). \quad (2)$$

Here, $a_0$ and $a_1$ are the attenuation volumes from the wall and working face, respectively; $K_{p,max}$ is the initial coefficient of the bulk; $d_0$ and $d_1$ are the attenuation volumes from point $(x, y)$ to the wall and working face, respectively (m$^{-1}$); $K_{p,min}$ is the compacted coefficient of the bulk; $\xi_1$ is the adjustment factor for controlling the distribution of the "O" model; and $K_p$ is the coefficient of the bulk.

### D. Temperature field of the goaf

The thermodynamic process in a goaf is very complex. The quantity of heat transferred via the roof, floor, and tunnels' sides cannot be measured. Moreover, the size of the rocks in a goaf is nonuniform. It is also difficult to describe the heat loss due to spontaneous combustion. The heat balance equation can be established based on the energy conservation equation as follows:[32,33]

$$C_e \dfrac{\delta T}{\delta t} + n\sigma_g\left(V_x \dfrac{\delta T}{\delta x} + V_y \dfrac{\delta T}{\delta y}\right) = Q_s + \lambda_e\left(\dfrac{\partial^2 T}{\partial x^2} + \dfrac{\partial^2 T}{\partial y^2}\right), \quad (3)$$

where $C_e$ is the effective heat capacity of the porous media, $C_e = n\sigma_g + (1-n)\sigma_s$ (J/m$^3$ °C); $\lambda_e$ is the equivalent thermal conductivity of the porous media, $\lambda_e = n\lambda_g + (1-n)\lambda_s$ (W/m °C); $\sigma_s$ and $\lambda_s$ are the equivalent multi-lumped heat capacity and thermal conductivity of the solid in the porous media, respectively; $\sigma_g$ and $\lambda_g$ are the equivalent multi-lumped heat capacity and thermal conductivity of the gas in the porous media, respectively; $n$ is the porosity; $V_x$ and $V_y$ are the filtration flow (m/s); and $Q_s$ is the oxidation heat release from the goaf residual coal (J/m$^3$ s).

### E. Oxygen consumption in the goaf

Coal samples from the working face of the Daxing coal mine were obtained in accordance with the sampling rules of coal
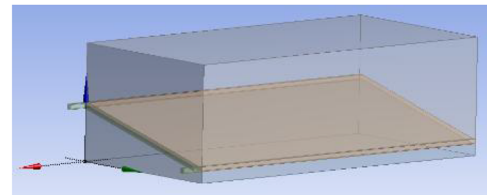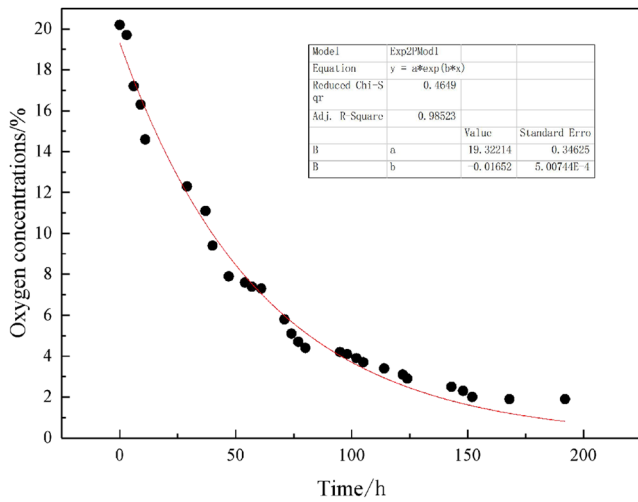


**FIG. 1**. Gob model.

FIG. 2. Variation in the oxygen concentration during coal oxidation.

spontaneous combustion testing. The test conditions were as follows: (1) the sample particle size is less than 2 cm, (2) the test temperature is 22 °C, (3) the volume of the reaction device is 5850 ml, (4) the sample weight is 3 kg, (5) the volume of air contained in the reaction device is 3542 ml, and (6) the pressure is 1.01 MPa. The device is completely sealed, and the monitoring time is 432 h. The experimental results are shown in Fig. 2.

The oxygen concentration curve can be fitted by the following equation:

$$c(\tau) = 19.322\,14 \cdot \ell^{-0.016\,52\tau}. \tag{4}$$

The oxygen consumption volume constant can be determined from the following equation:

$$\gamma_0 = c_0 \cdot V_0 \cdot \lambda_0 = 19.322\,14 \times 3.542 \times 10^{-3} \times 0.016\,52$$
$$= 1.13 \times 10^{-3}\,\mathrm{mol}/(\mathrm{m}^3\,\mathrm{s}). \tag{5}$$

Oxygen consumption is related to oxygen concentration, environmental temperature, particle size of the coal, air leak intensity, and stone volume.[34,35] The relationship between oxygen consumption and these factors can be derived as follows:

$$w_1(O_2) = \alpha_0 C_{O_2} \ell^{b_0 T}\left[1 - \alpha_1 \ln\left(\frac{d}{d'} + C\right)\right]\left[1 - \ell^{B_1(\varepsilon - 1)}\right]/1000, \tag{6}$$

where $w_1(O_2)$ is the coal oxygen consumption volume (kg/m$^3$ s); $\alpha_0$, $\alpha_1$, $b_0$, and $\beta$ are the undetermined coefficients, $C_0$ is the oxygen concentration (kg/m$^3$); $T$ is the temperature (°C); $D$ is the coal size; $d'$ is the referenced size; $C$ and $B_1$ are the regression parameters; $\bar{Q}$ is the air leak intensity (m$^3$/m$^2$ s); and $\varepsilon$ is the stone volume.

Because the gas is being used as a diluent, the decrease in the oxygen concentration can be expressed by the equivalent oxygen consumption volume. The equivalent oxygen consumption volume can be given by the following equation:

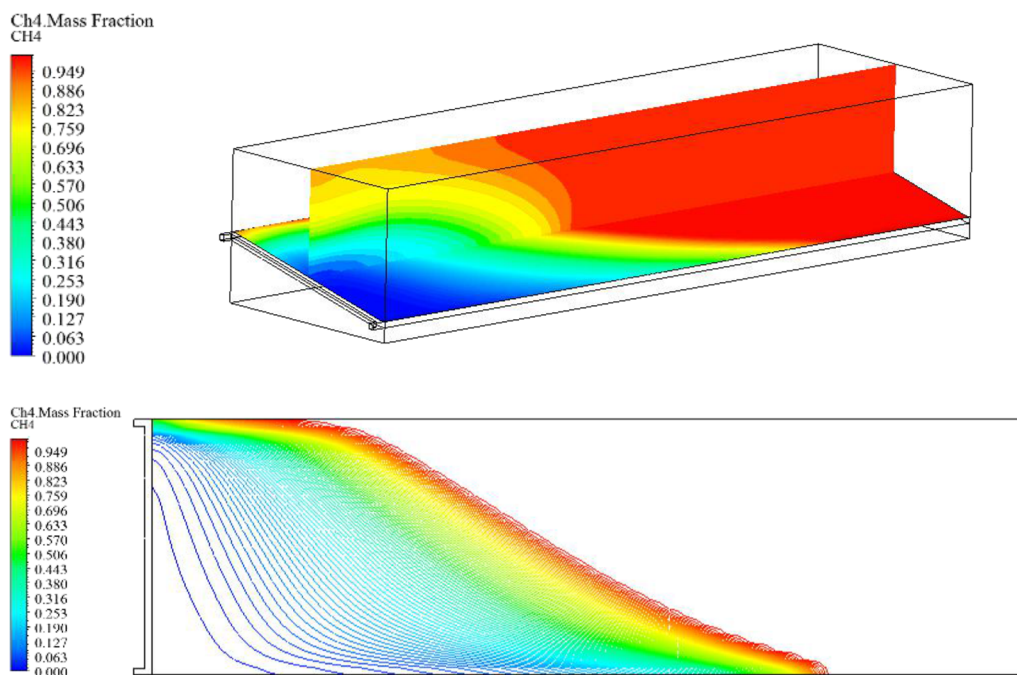$$w_2(O_2) = \frac{0.0224n \cdot w_g \cdot C_{O_2}}{n + 0.0112w_g}/1000. \tag{7}$$





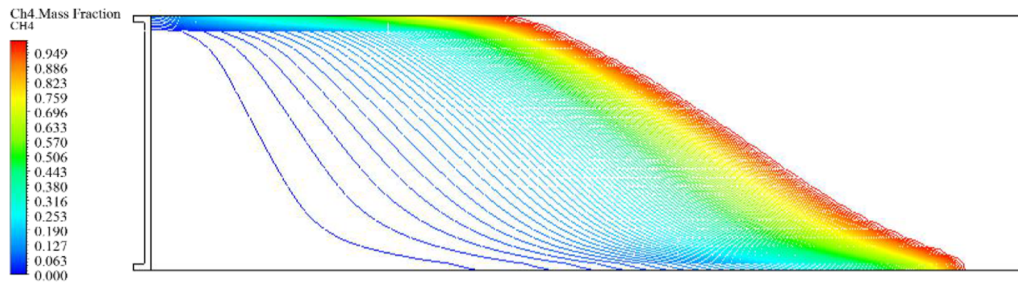FIG. 3. Gas concentration distribution in the goaf with an airflow of 300 m$^3$/min.

**FIG. 4**. Gas concentration distribution in the goaf with an airflow of 1400 m³/min.

Here, $w_2(O_2)$ is the equivalent volume of oxygen consumption (kg/m³ s), $C_{O_2}$ is the oxygen concentration before gas emission (kg/m³), $n$ is the porosity, and $w_g$ is the gas emission intensity (kg/m³ s).

The oxygen consumption in the goaf can be given by the following expression:

$$W(O_2) = w_1(O_2) + w_2(O_2). \qquad (8)$$

### F. Gas emission in the Daxing mine

The gas flows into the pores of the goaf. The relative gas emission volume of the working face is 24. 46 m³/t. The distribution of gas emission intensity in a unit area of the goaf can be described by the following equation:[29]

$$W(x,y) = \lambda \cdot \gamma \cdot q_T [\beta_1 M_1 (1 - \alpha_1) + \beta_2 (1 - \alpha_2)(M - M_1)] \cdot \ell^{-\lambda \frac{x}{v}}, \qquad (9)$$

where $x$ is the coordinate along the strike direction from the working face in the goaf (m), and $v$ is the advancing speed of the working face per day (m/d).

The average thickness of the coal seam in the Daxing coal mine is 5.1 m, the coefficient of recovery is 30%, the height of the shearer cutting is 3 m, the relative gas emission volume is 24.46 m³/t, the mining speed per day is 3 m, and the density of the coal is 1.46 t/m³. The gas emission intensity per unit area can thus be simplified as follows:

$$W(x,y) = 0.925\ell^{-0.025 \times} \text{ mol/(m}^2 \text{ s).} \qquad (10)$$

### G. Boundary conditions

The velocity inlet is selected as the air intake airway. The temperature is 293 K, oxygen volume fraction is 21%, nitrogen volume fraction is 79%, and absolute pressure is 101 325 Pa at the air intake. The outflow is selected for the return airway. The gasflow is assumed to be a laminar flow in the roof and the floor of the goaf and a turbulent flow in the goaf. The permeability of the porous media is given by Eq. (2). The gravity of the gas is considered because an evident floating phenomenon, induced by the density difference, will occur.

## III. ANALYSIS OF RESULTS

### A. Effect of the airflow at the working face on the gas migration in the goaf

A "U"-type ventilation is used in the Daxing coal mine. The gas concentration distribution in the goaf was obtained under different airflow conditions of 300 m³/min, 400 m³/min, 500 m³/min, 600 m³/min, 700 m³/min, 800 m³/min, 1000 m³/min, 1200 m³/min, 1400 m³/min, 1500 m³/min, 1600 m³/min, 1800 m³/min, 2000 m³/min, 2400 m³/min, 2800 m³/min, and 3000 m³/min. It can be concluded that the shape of gas concentration distribution basically remains consistent with increasing airflow, but the gas is blown deeper into the goaf. In addition, the gas concentration is higher at the side of the air intake airway in the goaf than at the side of the return airway due to the buoyancy of the gas. However, when the air leakage increases in the goaf, the gas exhausted from the goaf increases, and the gas concentration in the upper corner exceeds the acceptable limit. These results also demonstrate that it is impossible to solve the problem of excessively high gas concentration in the upper corner of a u-type ventilation system by increasing the airflow at the working face (Figs. 3 and 4).

The gas concentration distribution moves backward as a whole in the goaf with an increase in the airflow at the working face. The
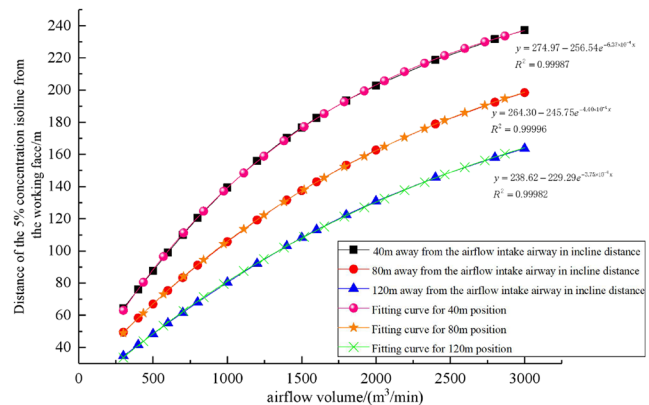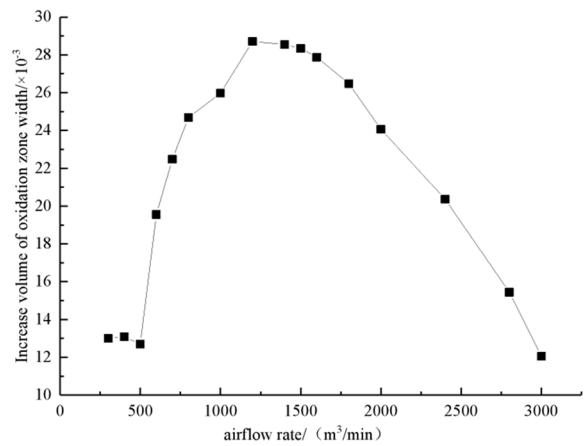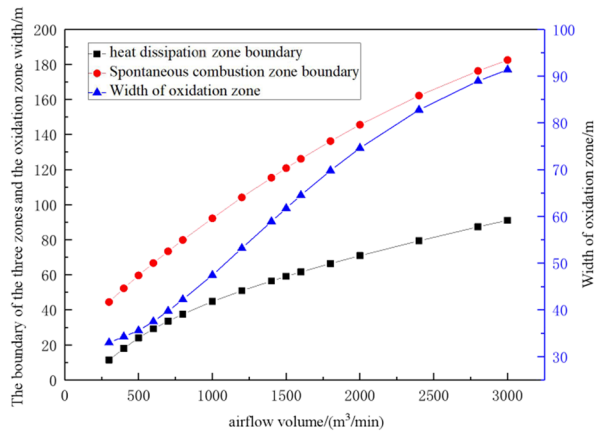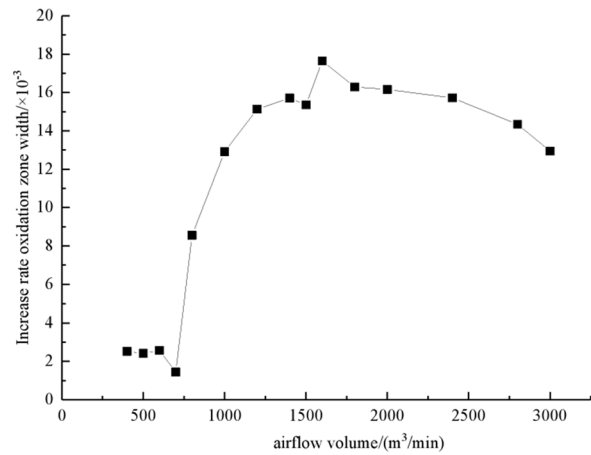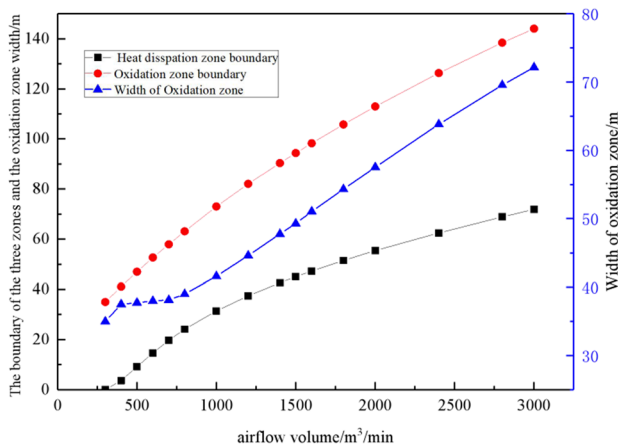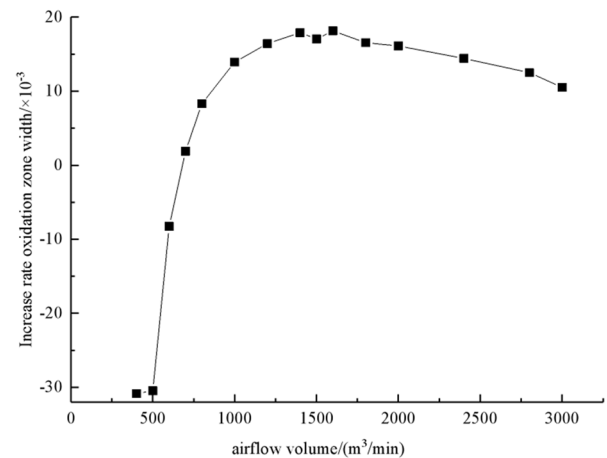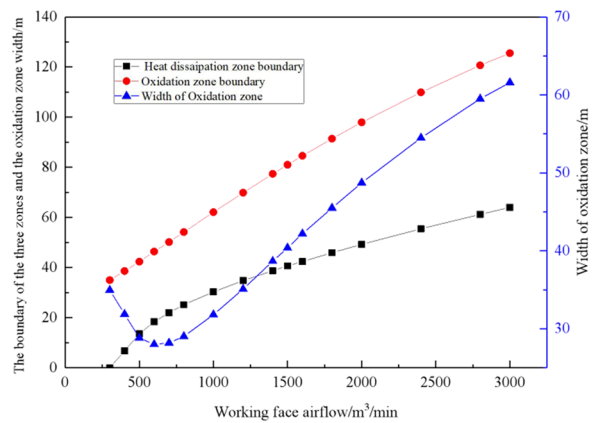


**FIG. 5**. Relationship between the position of the isoline corresponding to a gas concentration of 5% and the airflow volume.

*(a) 40 m*



*(b) 80 m*



*(c) 120 m*

FIG. 6. Change in the width of the oxidation zone with varying airflow volumes in different incline direction locations.
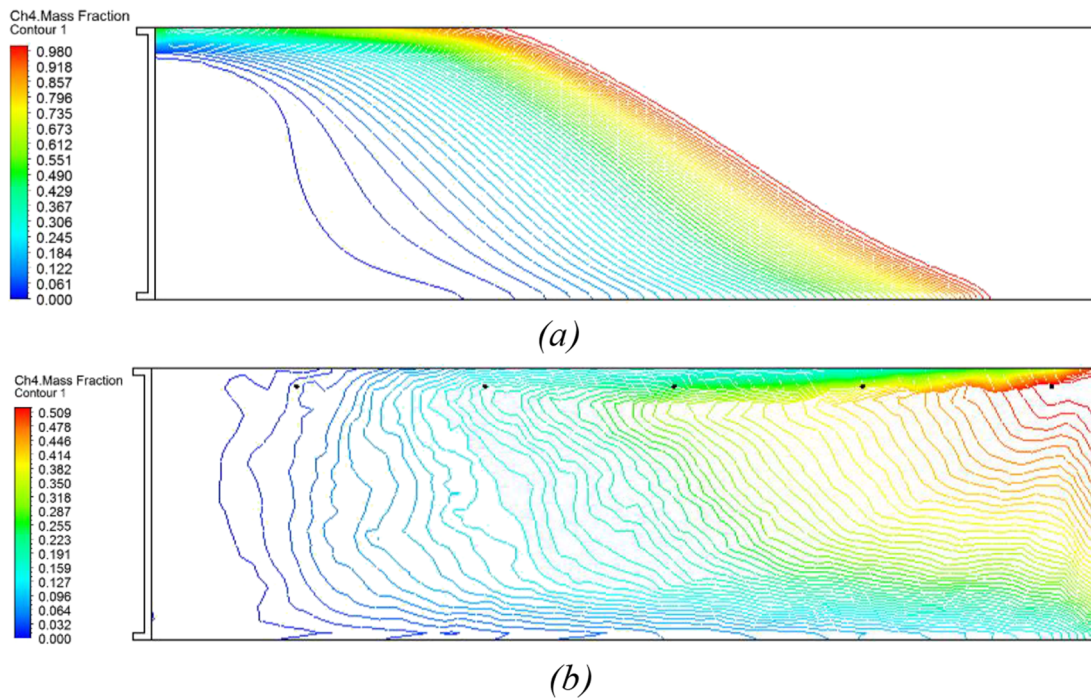
**FIG. 7**. Gas concentration distributions before and after surface drilling drainage with an airflow of 1000 m³/min: (a) gas concentration in the goaf before extraction and (b) gas concentration in the goaf after extraction.



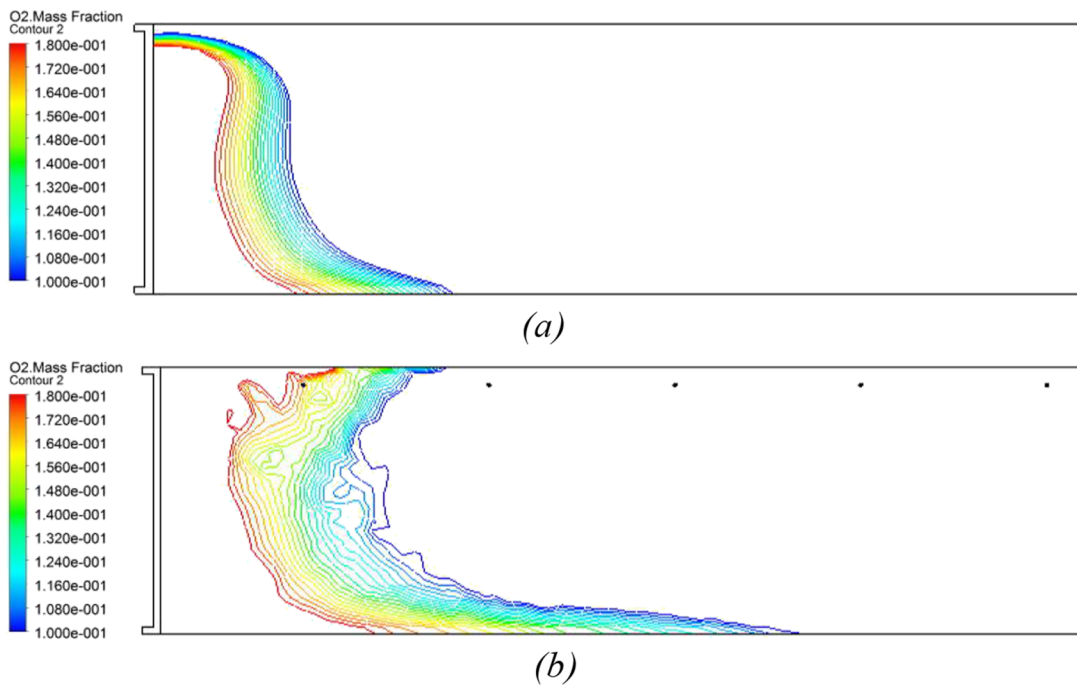**FIG. 8**. Oxygen concentration distributions before and after surface drilling drainage with an airflow volume of 1000 m³/minP: (a) oxygen concentration in the goaf before extraction and (b) oxygen concentration in the goaf after extraction.

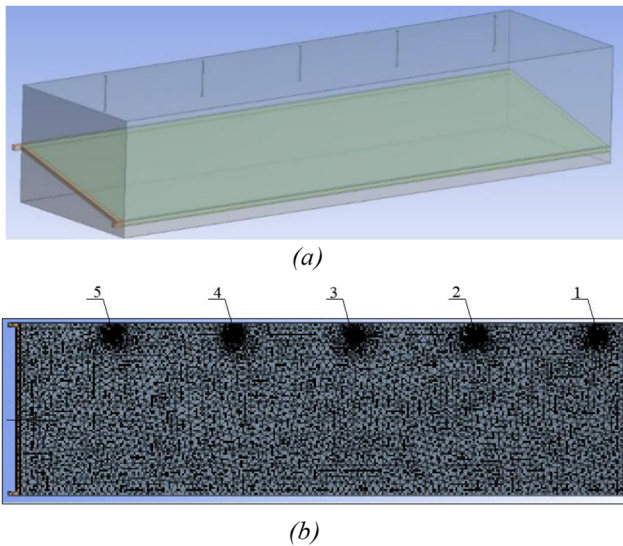**FIG. 9**. Surface drilling model: (a) stereogram and (b) meshing.

magnitude of the increase. This is beneficial for restraining gas emission out of the goaf.

## B. Relationship between the oxidation zone width and airflow

The air leakage intensity into the goaf, oxidation zone width in the goaf, and gas emission intensity from the goaf all increase with an increase in the airflow at the working face. The wider the oxidation zone width, the longer it takes to change from the oxidation zone to the suffocation zone. If this time exceeds the period of coal spontaneous combustion, the fire risk in the goaf will increase. Reasonable determination of the airflow at the working face can improve the ability of the ventilation system to prevent fires in the goaf.

The relationship between the airflow and oxidation zone width in the goaf was investigated in the Daxing coal mine. The shape of the oxidation zone does not change when the airflow at the working face increases. The results also indicate that the relationship between the oxidation zone width and the airflow at the working face is a quadratic function. However, when the airflow is less than 500 m³/min, the oxidation zone width has a simple linear relationship with the airflow at the center of the side of the return airway in the incline direction. The change in the oxidation zone width also has a quadratic relationship with the airflow (Fig. 6).

## C. Influence of the surface borehole drainage on gas migration and spontaneous combustion

Surface borehole drainage is mainly adopted compared with non-extraction. After gas extraction, the gas concentration in the

position of the isoline corresponding to a gas concentration of 5% moves backward exponentially with the increase in the airflow at the working face (Fig. 5). Although the tendency is the same in the inclined direction, the magnitude of the increase varies. The closer the distance to the air intake airway, the greater will be the



**FIG. 10**. Oxygen and gas concentration distribution for an extraction volume of 13.5 m³/min with drilling at borehole no. 1: (a) oxygen concentration distribution and (b) gas concentration distribution.
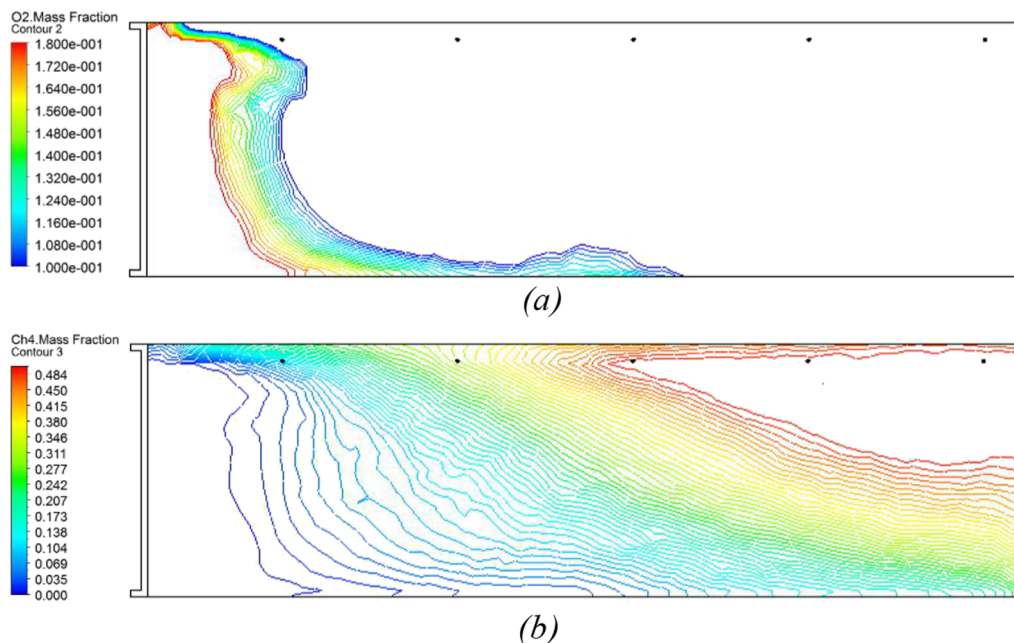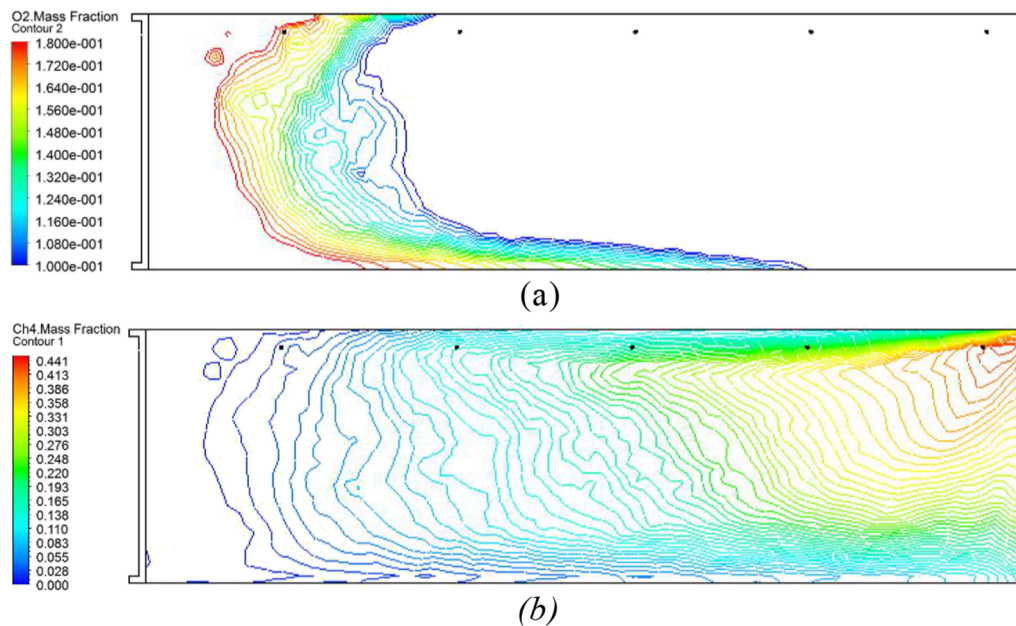
**FIG. 11**. Oxygen and gas concentration distribution for an extraction volume of 54 m$^3$/min with drilling at borehole no. 1: (a) oxygen concentration distribution and (b) gas concentration distribution.

goaf changes evidently. The high-concentration gas position moves backward, and the gas concentration on both sides of the goaf is lower after extraction (in Fig. 7). However, the gas extraction also causes a slower oxygen concentration gradient and increases the width of the oxidation zone (in Fig. 8).

To consider the influence of the position of the borehole on spontaneous combustion and gas concentration distribution, five boreholes are located at distances of 23 m, 123 m, 223 m, 323 m, and 423 m from the open-cut hole in the strike direction, denoted with nos. 1, 2, 3, 4, and 5, respectively (Fig. 9). Borehole no. 5 is located near the corner of the working face, which can reduce the gas concentration in the goaf at the back of the upper corner and prevent the upper corner gas concentration from exceeding acceptable limits. Borehole no. 1 is located near the open-cut hole, which is necessary for the best extraction effect. The extraction scheme is designed as follows: extraction at borehole no. 1 alone; borehole nos. 1 and 2 together; borehole nos. 1 and 3 together; borehole nos. 1 and 4 together; borehole nos. 1 and 5 together; borehole nos. 1, 2, and 5 together; and borehole nos. 1, 4, and 5 together. The extraction volume is 6. 75 m$^3$/min, 13. 5 m$^3$/min, 27 m$^3$/min, and 54 m$^3$/min.

The simulation results show that the width of the oxidation zone near the return airway initially changes when the extraction volume increases to 13.5 m$^3$/min during extraction at only borehole no. 1 ( Fig. 10). The oxidation zone width exceeds 100 m when the extraction volume increases to 54 m$^3$/min (in Fig. 11). The variation in the oxidation zone width is shown in Fig. 12 at 40 m, 80 m, and 120 m from the side of the air intake airway under different gas extraction volumes. The oxidation zone width increases with an increase in gas extraction volume, but it does not increase

significantly when the extraction volume is less than 15 m$^3$/min. However, the oxidation zone width increases sharply when the extraction volume exceeds 27 m$^3$/min. Thus, when the extraction volume is in the range of 13. 5 m$^3$/min to 27 m$^3$/min, by making the oxidation zone width change little, the gas extraction volume should be as small as possible.

A gas extraction volume of 27 m$^3$/min is applied to investigate the influence of the borehole locations on the effect of gas extraction. Using borehole nos. 1 and 2 for gas extraction simultaneously
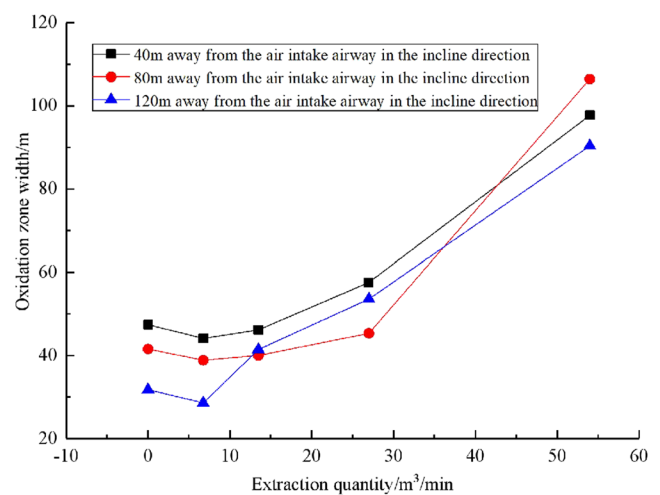


**FIG. 12**. Change in the oxidation zone width with drilling at borehole no. 1.

**FIG. 13**. Oxygen and gas concentration distribution for an extraction volume of 27 $m^3$/min with drilling at borehole nos. 1 and 2: (a) oxygen concentration distribution and (b) gas concentration distribution.
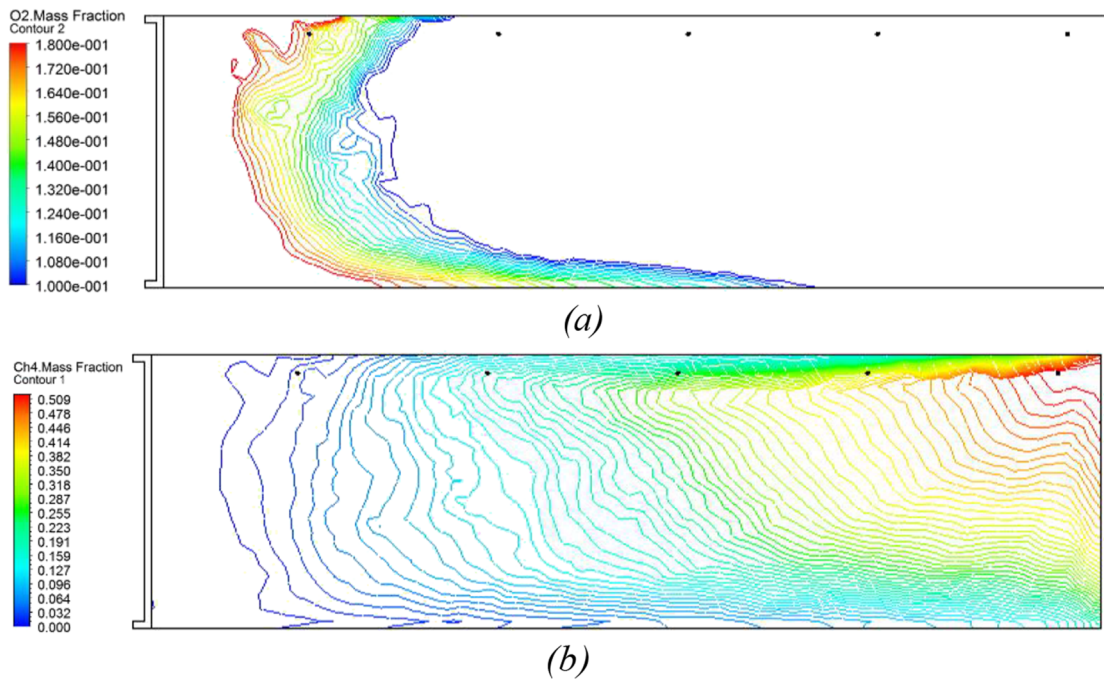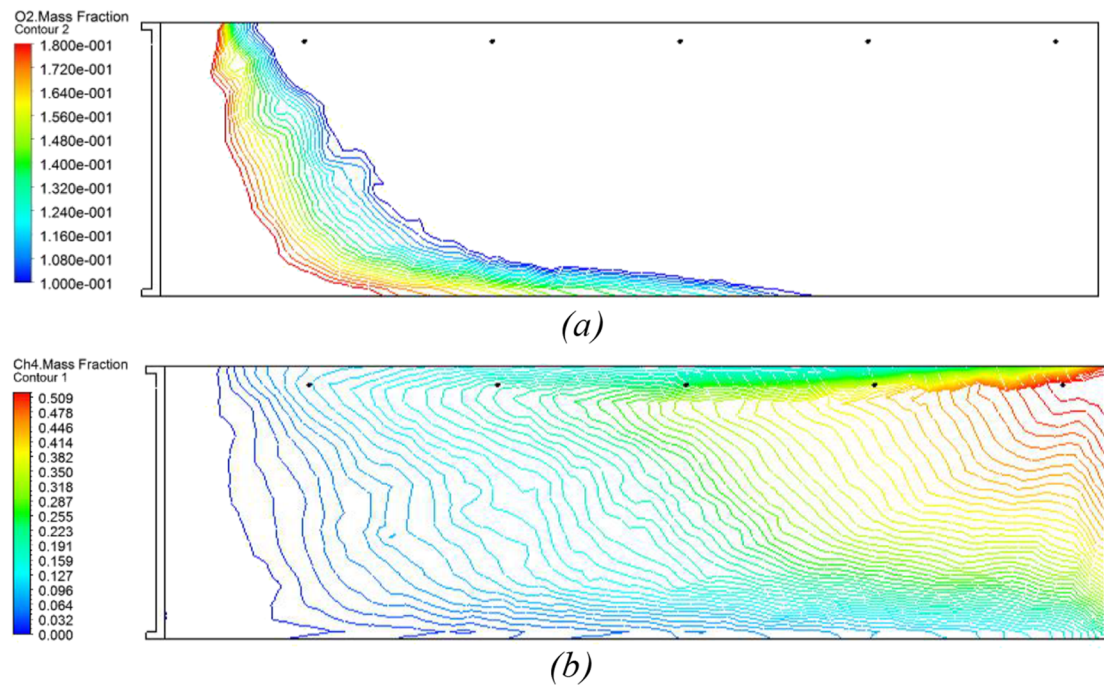


**FIG. 14**. Oxygen and gas concentration distribution for an extraction volume of 27 $m^3$/min with drilling at borehole nos. 1, 2, and 5: (a) oxygen concentration distribution and (b) gas concentration distribution.

is beneficial for reducing the gas depth in the goaf, but the gas concentration still exceeds the specified value in the upper corner (Fig. 13). When borehole nos. 1, 2, and 5 are used simultaneously, not only does the gas concentration deep in the goaf decreases but the gas concentration in the upper corner also decreases dramatically (Fig. 14).

## D. Optimal values for airflow volume, nitrogen injection, and gas extraction

Gas extraction and nitrogen injection are the most effective methods for preventing fires and gas disasters in a goaf. To investigate gas migration and spontaneous combustion under the conditions of simultaneous gas extraction and nitrogen injection in the goaf, borehole nos. 1, 2, and 5 are used for gas extraction; the location of nitrogen injection is 30 m from the working face, at which the airflow volume is 1000 $m^3$/min.

The simulation results are shown in Fig. 15 for the conditions of gas extraction and nitrogen injection. Gas extraction increases the

air leakage. The flow field is changed, and the oxidation zone width is reduced near the location of the nitrogen injection. However, nitrogen injection has little effect on the oxidation zone width near the center of the goaf and at the side of the return airway in the incline direction of the goaf. Thus, a narrow range from the center of the goaf to the side of the return airway becomes the main area for the occurrence of spontaneous combustion.

With borehole nos. 1, 2, and 5 used for gas extraction simultaneously, the airflow volume is set to 500 $m^3$/min, 1000 $m^3$/min, 1600 $m^3$/min, 2000 $m^3$/min, 2800 $m^3$/min, and 3000 $m^3$/min; the gas extraction volume is set to 13. 5 $m^3$/min, 27 $m^3$/min, and 54 $m^3$/min. It is shown in Figs. 16 and 17 that the width of the oxidation zone increases linearly with an increase in airflow volume and has a quadratic relationship with the gas extraction volume.

To investigate the comprehensive influence of the nitrogen injection location, nitrogen injection volume, and airflow volume, the nitrogen injection volume is varied to 600 $m^3$/h, 1200 $m^3$/h, and 1800 $m^3$/h. The nitrogen injection location is set at 10 m, 20 m, 30 m, and 40 m from the working face at the side of the air intake airway.
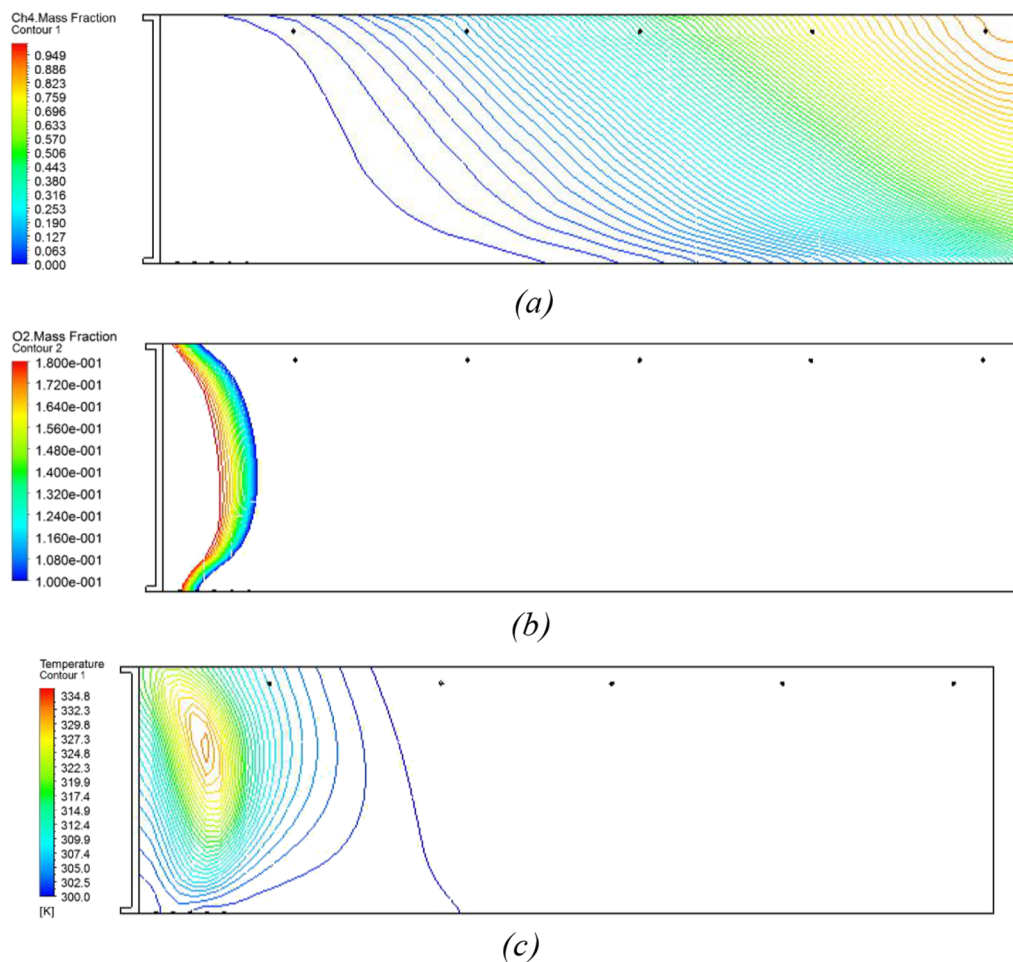


**FIG. 15**. Gas, oxygen distribution, and temperature field under the condition of drilling drainage combined with nitrogen injection: (a) gas concentration distribution, (b) oxygen concentration distribution and (c) temperature field.
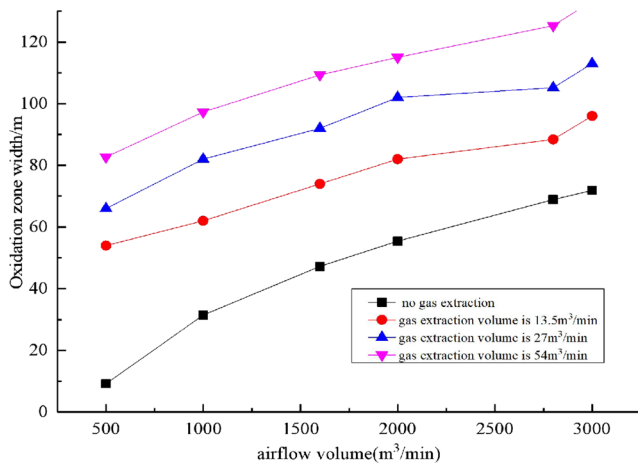
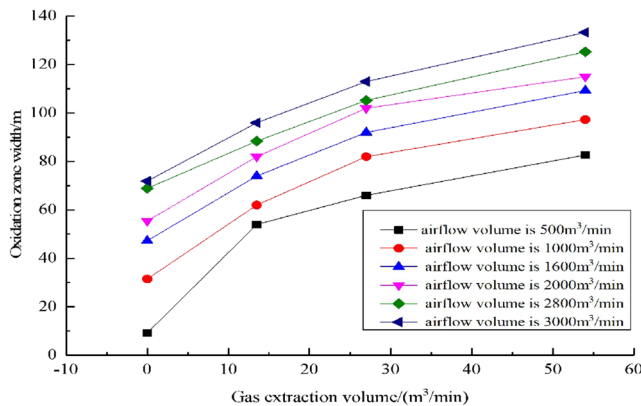FIG. 16. Width of the oxidation zone at different airflow volumes.



FIG. 17. Width of the oxidation zone at different gas extraction volumes.
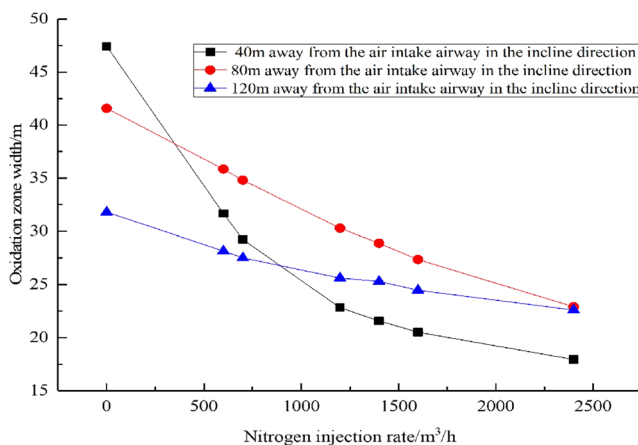


FIG. 18. Change in the oxidation zone width with varying nitrogen injection volumes.

TABLE I. Optimal values under conditions of different control measures.

| No. | Airflow volume ($m^3$/min) | Nitrogen injection volume ($m^3$/h) | Nitrogen injection location (m) | Gas extraction volume ($m^3$/min) |
|-----|------|------|-----|------|
| 1 | 500 | 720 | 20 | 13.5 |
| 2 | 1000 | 1200 | 30 | 13.5 |
| 3 | 1600 | 1200 | 30 | 27 |
| 4 | 2000 | 1800 | 30 | 27 |

The airflow volume is 1000 $m^3$/min, 1600 $m^3$/min, 2000 $m^3$/min, and 2800 $m^3$/min at the working face. The gas extraction volume is set to 13.5 $m^3$/min, 27 $m^3$/min, and 54 $m^3$/min.

Figure 18 shows a significant influence on the oxidation zone width when the nitrogen injection location is 10 m from the working face. The oxidation zone width decreases when the nitrogen injection rate reaches 1400–1600 $m^3$/h. However, when the nitrogen injection volume exceeds 1600 $m^3$/h, the amplitude of the decrease is reduced.

Through a large number of numerical simulations, the optimal values under the conditions of different control measures are determined for the Daxing coal mine and are listed in Table I.

## IV. CONCLUSION

Computational fluid dynamics technology is used to calculate the optimal value of parameters related to fire and gas prevention measures. It is helpful for mine managers to understand the characteristics of goaf flow clearly and to determine the best design plan that can support management decisions. This study is based on simulations, considering the actual situation of the Daxing Mine in Liaoning Province. The following conclusions can be drawn:

The shape of the gas concentration distribution remains basically consistent in the goaf with an increase in airflow volume at the working face. The gas concentration distribution as a whole moves toward the depth of the goaf, and the gas concentration near the working face in the goaf decreases markedly. The gas concentration does not evidently decrease in the upper corner with an increase in airflow volume at the working face. Thus, it is impossible to solve the gas problem in the upper corner with a u-type ventilation by increasing the airflow volume.

The optimal values of comprehensive parameters such as airflow volume, gas extraction volume, and nitrogen injection volume and location are analyzed for the Daxing coal mine. The nitrogen injection location, nitrogen injection volume, and gas extraction volume under different airflow volumes are optimized. With an increase in airflow volume, the nitrogen injection volume should gradually increase, and the location of the nitrogen injection can be increased to 30 m. The gas extraction volume should remain within the range of 13.5–27 $m^3$/min.

The data that support the findings of this study are available from the corresponding author upon reasonable request.

## REFERENCES

[1] K. Gao, J. Deng Li, and Z. Liu, "Study on mine ventilation resistance coefficient inversion based on genetic algorithm," Arch. Min. Sci. **63**(4), 813–826 (2018).

[2] B. Qin, L. Li, D. Ma, Y. Lu, X. Zhong, and Y. Jia, "Control technology for the avoidance of the simultaneous occurrence of a methane explosion and spontaneous coal combustion in a coal mine: A case study," Process Saf. Environ. Prot. **103**, 203–211 (2016).

[3] B. Zhou Fu, "Coexistence of gas and coal spontaneous combustion research: Disaster mechanism," J. Coal **5**, 843–849 (2012).

[4] S. Wu, Z. Jin, and C. Deng, "Molecular simulation of coal-fired plant flue gas competitive adsorption and diffusion on coal," Fuel **239**, 87–96 (2019).

[5] Y.-t. Liang and S.-g. Wang, "Prediction of coal mine goaf self-heating with fluid dynamics in porous media," Fire Safety J. **87**, 49–56 (2017).

[6] C. Zheng, M. S. Kizil, Z. Chen, and S. M. Aminossadati, "Effects of coal properties on ventilation air leakage into methane gas drainage boreholes: Application of the orthogonal design," J. Nat. Gas Sci. Eng. **45**, 88–95 (2017).

[7] R. K. Pan, C. Lu, K. Yang *et al.*, "Distribution regularity and numerical simulation study on the coal spontaneous combustion "three zones" under the ventilation type of ventilation type of Ч + J," Procedia Eng. **26**, 704–711 (2011).

[8] Q.-w. Deng, X.-h. Liu, C. Lu *et al.*, "Numerical simulation of spontaneous oxidation zone distribution in goaf under gas stereo drainage," Procedia Eng. **52**, 72–78 (2013).

[9] W. Liu and Y. Qin, "A quantitative approach to evaluate risks of spontaneous combustion in longwall gobs based on CO emissions at upper corner," Fuel **210**, 359–370 (2017).

[10] T. Chu, P. Li, and Y. Chen, "Risk assessment of gas control and spontaneous combustion of coal under gas drainage of an upper tunnel," Int. J. Min. Sci. Technol. **29**, 491–498 (2019).

[11] J. Zhao, J. Deng, J. Song, and C.-M. Shu, "Effectiveness of a high-temperature-programmed experimental system in simulating particle size effects on hazardous gas emissions in bituminous coal," Safety Sci. **115**, 353–361 (2019).

[12] T. Zhou Ai, K. Wang, J. Zang, Z. Yan Ben, and K. Lu, "Numerical simulation of gas and fire co-governance in goaf prone to spontaneous combustion," Chin. J. Safety Sci. **20**(8), 49–53 (2010).

[13] C. Ting-xiang, Z. Shi-xuan, X. Yong-liang, and Z. Zhi-jun, "Research on the coupling effects between stereo gas extraction and coal spontaneous combustion," Procedia Eng. **26**, 218–227 (2011).

[14] M. Tang, B. Jiang, R. Zhang, Z. Yin, and G. Dai, "Numerical analysis on the influence of gas extraction on air leakage in the gob," J. Nat. Gas Sci. Eng. **33**, 278–286 (2016).

[15] J. Zhang, J. An, Z. Wen, K. Zhang, R. Pan, and N. Akter Al Mamun, "Numerical investigation of coal self-heating in longwall goaf considering airflow leakage from mining induced crack," Process Saf. Environ. Prot. **134**, 353–370 (2020).

[16] Y. Liang, J. Zhang, L. Wang, H. Luo, and T. Ren, "Forecasting spontaneous combustion of coal in underground coal mines by index gases: A review," J. Loss Prevent. Process Ind. **57**, 208–222 (2019).

[17] K. Gao, M. Liu Zi, and Z. Jia Jin, "Study on flame spread characteristics of flame-retardant cables in mine," Adv. Polym. Technol. **10**, 1–8 (2020).

[18] C. Liu, G. Li Shu, and G. Yang Shou, "Gas emission quantity prediction and drainage technology of steeply inclined and extremely thick coal seams," Int. J. Min. Sci. Technol. **20**, 415–422 (2018).

[19] H. Liu, Y. Cheng, H. Chen, J. Mou, and S. Kong, "Characteristics of mining gas channel expansion in the remote overlying strata and its control of gasflow," Int. J. Min. Sci. Technol. **23**, 481–487 (2013).

[20] Y. Song, S. Yang, X. Hu, W. Song, N. Sang, J. Cai, and Q. Xu, "Prediction of gas and coal spontaneous combustion coexisting disaster through the chaotic characteristic analysis of gas indexes in goaf gas extraction," Process Saf. Environ. Prot. **129**, 8–16 (2019).

[21] W. Cheng, X. Hu, J. Xie, and Y. Zhao, "An intelligent gel design to control the spontaneous combustion of coal: Fire prevention and extinguishing property," Fuel **210**, 826–835 (2017).

[22] K. Gao, S. N. Li, R. Han *et al.*, "Study on the propagation law of gas explosion in the space based on the goaf characteristic of coal mine," Safety Sci. **127**, 104693 (2020).

[23] J. Fan Yi, Y. Zhao Yan, M. Hu Xiang, Y. Wu Ming, and D. Xue, "A novel fire prevention and control plastogel to inhibit spontaneous combustion of coal: Its characteristics and engineering applications," Fuel **263**, 116693 (2020).

[24] M. Onifade and B. Genc, "Spontaneous combustion of coals and coal-shales," Int. J. Min. Sci. Technol. **28**, 933–940 (2018).

[25] J. Guo, H. Wen, X. Zheng, Y. Liu, and X. Cheng, "A method for evaluating the spontaneous combustion of coal by monitoring various gases," Process Saf. Environ. Prot. **126**, 223–231 (2019).

[26] B. Taraba, Z. Michalec, V. Michalcoava, T. Blejchar, M. Bojko, and M. Kozubkova, "CFD simulations of the effect of wind on the spontaneous heating of coal stockpiles," Fuel **118**, 107–112 (2013).

[27] J. Zhang, Y.-t. Liang, Z. Ren, Z.-w. Wang, and G.-d. Wang, "Transient CFD modelling of low-temperature spontaneous heating behaviour in multiple coal stockpiles with wind forced convection," Fuel Process. Technol. **149**, 55–74 (2016).

[28] M. V. Kok, "Simultaneous thermogravimetry-calorimetry study on the combustion of coal samples: Effect of heating volume," Energy Convers Manag. **53**(1), 40–44 (2012).

[29] F. Yang, Y. Lai, and Y. Song, "Determination of the influence of pyrite on coal spontaneous combustion by thermodynamics analysis," Process Saf. Environ. Prot. **129**, 163–167 (2019).

[30] K. Hooman and U. Maas, "Theoretical analysis of coal stockpile self-heating," Fire Safty J. **67**, 107–112 (2014).

[31] B. Moghtaderi, B. Z. Dlugogorski, and E. M. Kennedy, "Effects of wind flow on self-heating characteristics of coal stockpiles," Process Saf. Environ. Prot. **78**, 445–453 (2000).

[32] M. Krajčiová, L. Jelemenský, M. Kiša, and J. Markoš, "Model predictions on self-heating and prevention of stockpiled coals," J. Loss Prevent. Process Ind. **17**, 205–216 (2004).

[33] V. Fierro, J. L. Miranda, C. Romero, J. M. Andrés, A. Arriaga, and D. Schmal, "Model predictions and experimental results on self-heating prevention of stockpiled coals," Fuel **80**, 125–134 (2001).

[34] F. Guorui and P. Wang, "Simulation of recovery of upper remnant coal pillar while mining the ultra-close lower panel using longwall top coal caving," Int. J. Min. Sci. Technol. **30**, 55–61 (2020).

[35] W. Lu, Y.-J. Cao, and J. C. Tien, "Method for prevention and control of spontaneous combustion of coal seam and its application in mining field," Int. J. Min. Sci. Technol. **27**, 839–846 (2017).